

Effect of alloyed target vis-à-vis pure target on machining performance of TiAlN coating

Paranjayee Mandal · S. Paul

Received: 13 August 2011 / Accepted: 26 June 2012
© Springer-Verlag London Limited 2012

Abstract Typically closed-field unbalanced magnetron sputtering (CFUBMS) and controlled cathodic arc deposition techniques having four or six pure or alloyed targets are employed for commercial titanium aluminium nitride (TiAlN) coating of cutting tools. The role of the use of alloyed target vis-à-vis pure target on the coating characteristics and the machining performance of TiAlN-coated tools has not been studied in detail. In the present work, TiAlN coating has been deposited on cutting tools using a pulsed DC, dual-cathode CFUBMS system to capture the role of the type of target on machining performance. The deposition rate in the case of the alloyed target has been found to be much higher as compared to the pure target. Such coatings deposited from alloyed targets also provided significantly better machining performance in dry turning of low-carbon and high-carbon steel. Dry turning of SAE 1070 high-carbon steel at 160 m/min did not yield more than 100 μm of average flank wear on the same insert coated using alloyed targets for a machining time of more than 3 min.

Keywords TiAlN coating · Pulsed DC closed-field unbalanced magnetron sputtering · Pure target · Alloyed target · Machining performance

1 Introduction

Physical vapour deposition (PVD)-coated cutting tools are very efficient in enhancing productivity in the metal cutting

industry. They are preferred over chemical vapour deposition (CVD)-coated cutting tools owing to the lower deposition temperature (300–500 °C). The most common are the titanium nitride (TiN)-coated tools, which are widely used as protective hard coating to increase the lifetime and performance of cutting and forming tools. Munz [1] reported that the main drawback of TiN-coated tools is that they are easily oxidized at 550 °C and form poor adherent and a brittle titanium dioxide (TiO₂) layer on top of the TiN layer. Because of the large difference in the molar volume of TiO₂ and TiN, compressive stresses are developed in the oxide layers and spallation takes place. Therefore, the protecting ability of the TiN coating is lost. To overcome such a problem and to improve the mechanical properties of TiN coating, the incorporation of a third element, like Al, Si, Cr, or Zr, to the TiN film has been suggested to form a ternary composite coating so that the new multicomponent films can yield superior oxidation resistance and increase the tool life significantly compared to conventional TiN coating. Lee et al. [2] have studied the effect of the incorporation of Cr on the structure and properties of titanium chromium nitride ((TiCr)N) coating and inferred that an increase in Cr content led to a beneficial effect on wear resistance and coating hardness. Santana et al. [3] have reported that the addition of Al enhances the thermal stability of TiAlN coating.

Since the mid 1980s, TiAlN coating had been successfully developed as a promising alternative to TiN-coated cutting and forming tools. Munz [1] developed TiAlN coating using sputter ion-plating process and reported the performance of TiAlN-coated drills to be two times better than that of TiN-coated ones. In recent years, TiAlN coating has been given much attention because of its high anti-oxidation property (it is oxidized at 800 °C), high hardness, high corrosion resistance and lower thermal conductivity, as reported by Munz [1]. McIntyre et al. [4] experimentally investigated the kinetics and mechanism of the oxidation of

P. Mandal (✉) · S. Paul
Department of Mechanical Engineering,
Indian Institute of Technology Kharagpur,
Kharagpur 721 302, West Bengal, India
e-mail: 200712mum@gmail.com

S. Paul
e-mail: spaul.mech@iitkgp.ernet.in

72 TiAlN films and observed that when the TiAlN film is
 73 exposed to high temperatures, it reacts with oxygen and
 74 forms a dense, highly adhesive aluminium oxide (Al_2O_3)
 75 layer on top of the coating, protecting it from further oxida-
 76 tion. Thus, TiAlN film exhibits good anti-oxidation behav-
 77 iour that helps in reducing adhesive wear, which is the major
 78 wear mechanism in the cutting tool. Another major advant-
 79 age of the TiAlN coating is its lower thermal conductivity,
 80 as cited by Hsieh et al. [5], which helps in the dissipation of
 81 more heat via chip. Therefore, thermal loading on the sub-
 82 strate reduces permitting higher cutting speeds.

83 Closed-field unbalanced magnetron sputtering (CFUBMS)
 84 using pure DC and pulsed DC, and controlled cathodic arc
 85 deposition of TiAlN have been well-researched areas. Kelly et
 86 al. [6] commented that the advent of pulsed DC CFUBMS
 87 could successfully address the issues of low deposition rate
 88 and target poisoning effectively whilst experimentally investi-
 89 gating the reactive unbalanced magnetron sputtering of alu-
 90 minium oxide coating. Most researchers have used four or six
 91 target machines using DC or the pulsed DC CFUBMS techni-
 92 que for the deposition of TiAlN. They have used both pure
 93 as well as alloyed targets. However, a survey of previous
 94 literature could not yield much information on TiAlN coating
 95 developed using dual-cathode deposition systems employing
 96 pulsed DC, reactive closed-field unbalanced magnetron sput-
 97 tering with pure and alloyed targets.

98 A survey of previous technical papers in the public do-
 99 main indicates the availability of little systematic informa-
 100 tion regarding the machining performance of TiAlN-coated
 101 tools whilst turning carbon steels. Jindal et al. [7] used PVD-
 102 coated TiN, titanium carbo-nitride (TiCN) and TiAlN-coated
 103 cemented carbide tools and compared their machin-
 104 ing performance whilst turning SAE 1045 medium-carbon
 105 steel at cutting velocities of 305 and 396 m/min, feed of
 106 0.15 mm/rev and depth of cut of 0.75 mm under a wet
 107 machining environment. The tool life criteria used have
 108 been average flank wear, VB , of 0.4 mm or maximum flank
 109 wear, VB_{max} , of 0.75 mm. They found the average flank
 110 wear to be only 0.2 mm after 60 min of machining when the
 111 cutting velocity was 305 m/min, but the tool life was only
 112 25 min when the cutting velocity was raised to 396 m/min
 113 for TiAlN-coated carbide inserts. Khrais and Lin [8] used
 114 commercial PVD-applied TiAlN-coated cemented carbide
 115 inserts (6 % cobalt) for turning AISI 4140 steel at a cutting
 116 velocity of 210–410 m/min, feed of 0.14 mm/rev and depth
 117 of cut of 1 mm under both wet and dry cutting conditions.
 118 They reported that with the increase in cutting speed from
 119 210 to 410 m/min, tool life decreased from 65 to 5 min.
 120 TiAlN-coated tools performed best under dry cutting for a
 121 cutting speed of <260 m/min.

122 Moreover, information regarding the comparison of the
 123 machining performance of TiAlN-coated inserts deposited
 124 from pure targets as well as alloyed targets has not been

found. Thus, the objective of the present study was to
 investigate the role of alloyed targets vis-à-vis pure targets
 on the characteristics and machining performance of TiAlN
 coating deposited in a dual-cathode pulsed DC CFUBMS
 system whilst turning different carbon steels.

2 Experimental details

TiAlN coating was deposited in a dual-cathode pulsed DC,
 closed-field unbalanced magnetron system (VTC-01A)
 manufactured by Milman Thin Film Systems Pvt. Ltd.,
 India. The coating system is shown photographically in
 Fig. 1. Coating had been deposited on three different types
 of substrates, namely, HSS block of M2 grade ($10 \times 10 \times$
 20 mm), low-carbon steel (SAE 1010) disc-shaped coupons
 $(\phi=25 \times 10$ mm) and uncoated tungsten carbide inserts of
 grade K10 (94 % WC+6 % Co) and nominal geometry
 SNMA 120408. Prior to deposition, all substrates except
 the inserts were polished to a roughness of $R_a=0.05 \mu m$
 and ultrasonically cleaned using acetone, trichloroethylene,
 isopropyl alcohol and distilled water. Before transferring the
 samples to the deposition chambers, they were dried using
 hot air. For three samples (S7, S8 and S9), one pure titanium
 and one pure aluminium target were used, whereas for two
 samples (S10 and S11) alloyed titanium–aluminium targets
 (atomic ratio Ti/Al=60:40) were used. All the targets had
 purity better than 99.99 %, with a dimension of $254 \times$
 127 mm and a thickness of 12 mm. The substrate stage
 had a twofold rotation facility and was imparted a rotational
 speed of 4 rpm during deposition. Bipolar pulsed DC power
 supplies (Advanced Energy Pinnacle Plus) were used. Cath-
 odes were energized in current mode and the substrate



Fig. 1 Photograph of the coating system

energized in voltage mode. A base pressure of better than 2×10^{-3} Pa was achieved prior to initiating deposition, which is very similar to the base pressure reported by Musil and Hruby [9] and Zhou et al. [10].

The deposition cycle consisted of sputter cleaning of the targets with shutters in closed position, followed by ion etching. Ion etching was conducted at a bias voltage of -500 V with a pulsed frequency of 250 kHz at Ar pressure of 0.16 Pa, with the titanium target current set to 1 A. Then, a titanium interlayer of around 200 -nm thickness (for S7, S8 and S9) or a titanium–aluminium interlayer (for S10 and S11) was deposited. This was followed by a TiN interlayer for samples S7, S8 and S9. Other relevant deposition parameters are given in Table 1.

The surface morphology and the fractograph of the coated samples were observed under a scanning electron microscope (Carl Zeiss EVO 60) fitted with an energy-dispersive X-ray (EDX) analyser (INCA FET 3X). The composite Vicker’s micro-hardness of the coating was measured using a load of 1 N with a dwell time of 15 s in a LECO LM-700 micro-hardness measurement system. For each sample, ten measurements were taken; their average has been reported.

The adhesion of the coating to the substrate has been measured by a TR-101 M5 DUCOM Scratch Tester with five replicates. Testing was undertaken with a Rockwell C diamond indenter having a tip radius of 0.2 mm. The indenter was drawn across the coating at a speed of 6 mm/min over a scratch length of 15 mm. The normal load during scratching was varied from 10 to 120 N.

The scratch adhesion is quantified by the normal load at which the coating fails. This is typically termed as the critical load or L_C . In the present work, the critical load has been determined by the sudden increase in the ratio of the tangential or traction force to the normal force during scratching. This typically coincides with the L_{C3} type of failure which indicates initiation of removal of the coating

from the scratch, as has been reported by He et al. [11]. All the above tests were performed on coated HSS M2 samples.

Ball-on-disc tests were performed using a tribometer (TR-201 M3 DUCOM) to study the tribological performance of the coating. The tests were undertaken at a normal load of 10 N using 5 -mm diameter cemented carbide balls (WC=94 % and Co=6 %) with a sliding speed of 200 mm/s under ambient conditions (25 °C and 50 % relative humidity). The depth of the wear track was measured at five different locations using contact-type surface profilometer (Taylor-Hobson Surtronic 3+).

The machining performance of the coated tungsten carbide inserts was evaluated by dry turning of as-rolled and proof-machined, low-carbon steel (SAE 1020 with 143 BHN) and annealed and proof-machined, high-carbon steel (SAE 1070 with 198 BHN) bars. The choice of high-carbon steel for the evaluation of cutting performance is common as high-carbon steels are difficult to machine. On the other hand, the problem with low-carbon steel is its ductility and toughness. Many of the previous researchers [12–15] had also used low-carbon steels for estimating the machining performance of coated (PVD/CVD) cutting tools. Hence, these two types of work materials have been chosen to evaluate the machining performance of TiAlN-coated inserts in the present study. Table 2 lists all the machining parameters. Machining was interrupted at regular intervals, and the rake and flank faces of the cutting tool were inspected under a stereo zoom microscope (Olympus model SZ 1145TR PT zoom stereomicroscope) fitted with a digital photomicrograph system (Olympus C-5060 wide zoom). The cutting tools were ultrasonically cleaned in acidic solution before such inspection to remove any work material built-up on the rake face. The average and the maximum flank wears were determined from the photomicrographs.

Normally, P-grade uncoated carbide inserts are used to machine steels because they are diffusion-resistant due to the presence of titanium carbide (TiC), tantalum carbide (TaC) and niobium carbide (NbC). K-grade uncoated inserts (plain WC inserts without any alloying carbides) are used in machining grey cast iron and nonferrous metals. The deposition of coating leads to a reduction in toughness or transverse rupture strength, particularly for CVD coating [16]. Therefore, to obtain an adequate balance between toughness and hardness of the cutting tool insert, tough and wear-resistant K-grade inserts are generally coated [7,16,17].

3 Results and discussion

Figure 2 shows the surface morphology and the fractograph of representative coatings, namely, S8, S10 and S11. The SEM photographs depicting the surface morphology have been acquired at $\times 10,000$, whereas the SEM photographs revealing the fractographs are at $\times 3,000$. This strategy has

t1.1 **Table 1** Deposition parameters for as-deposited TiAlN coating

t1.2	Ar flow rate	15 sccm
t1.3	N ₂ flow rate	10 sccm
t1.4	Chamber pressure of Ar	0.20 Pa
t1.5	Partial pressure of N ₂	0.07 Pa
t1.6	Ti target current (for pure target)	3 A
t1.7	Al target current (for pure target)	4 A
t1.8	Ti:Al target current (for alloyed target)	5 A
t1.9	Substrate bias voltage	-50 V
t1.10	Deposition temperature	300 °C (S8, S9)
t1.11		350 °C (S7, S10, S11)
t1.12	Target frequency	200 kHz (S8, S10)
t1.13		250 kHz (S7)
t1.14		300 kHz (S9, S11)
t1.15	Duty cycle	80 %

Table 2 Detailed machining parameters for dry turning

t2.1	Work material	SAE 1020 and SAE 1070 steel	
t2.2	Chemical composition	SAE 1020 steel	SAE 1070 steel
t2.3	of work material as	0.19 % C, 0.074 % Si, 0.374 % Mn,	0.716 % C, 0.223 % Si, 0.74 % Mn,
t2.4	provided by optical	0.043 % P, 0.03 % S, 0.02 % Cr,	0.018 % P, 0.022 % S, 0.003 % Cr,
	emission spectroscopy	rest Fe	rest Fe
t2.5	Inserts used	TiAlN-coated carbide (coated in-house)	
t2.6	Substrate grade	K10	
t2.7	Insert designation	SNMA 12 04 08	
t2.8	Tool holder specification	PSBNR 2525M12	
Q4 t2.9	Tool geometry	−6°, −6°, 6°, 6°, 15°, 75°, 0.8 (mm)—orthogonal rake system	
t2.10	Cutting velocity (m/min)	250 (for SAE 1020 steel)	
t2.11		160 (for SAE 1070 steel)	
t2.12	Feed (mm/rev)	0.2	
t2.13	Depth of cut (mm)	2	
t2.14	Environment	Dry	

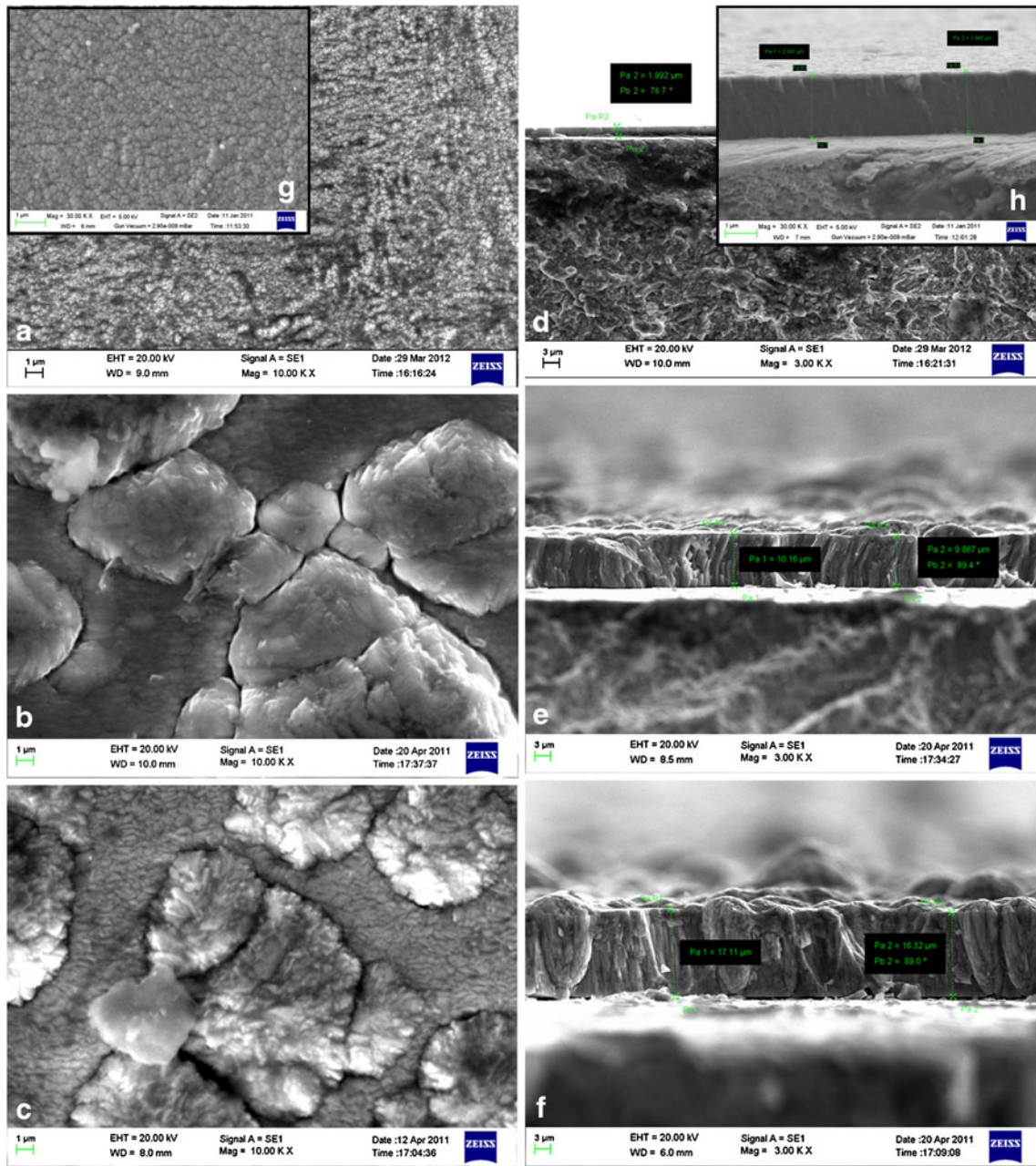
240 been adopted to clearly reveal interesting features on the
 241 surface and on the fractograph. The coating morphology of
 242 the S8 sample deposited from pure target looks finer; hence,
 243 an inset SEM photograph (Fig. 2g) has been added at ×30,000
 244 to clearly reveal the morphology. Similarly, the coating thick-
 245 ness on sample S8 is much smaller as compared to the coating
 246 thickness obtained on samples S10 and S11. Thus, an
 247 inset SEM photograph (Fig. 2h) has been added for sam-
 248 ple S8 at ×30,000. For sample S8, which has been depos-
 249 ited from pure targets, the agglomerated grain size seems
 250 to be sub-micronic, as can be seen in Fig. 2g. The coating
 251 also looks very compact both in the top view (Fig. 2g)
 252 and the fractograph (Fig. 2h). Similar compact nanocrys-
 253 talline coatings have been reported by Bhaduri et al. [19]
 254 for TiN deposited using dual-cathode reactive CFUBMS.
 255 The fractograph (Fig. 2h) reveals a dense columnar struc-
 256 ture, though it may not be termed as featureless, which
 257 was once again reportedly obtained for TiN coating at
 258 high negative bias voltage by Bhaduri et al. [19]. On the other
 259 hand, the samples (S10 and S11) obtained using alloyed
 260 targets provided much thicker coatings for the same coating
 261 cycle duration. But the coating consisted of large overgrowths,
 262 as can be seen in Fig. 2b, c. The fractographs (Fig. 2e, f) also
 263 reveal a clear columnar structure which did not resemble
 264 dense coating. The higher coating thickness for alloyed targets
 265 may be attributed to the higher target current density. Further-
 266 more, in the case of pure targets, the dual-cathode configura-
 267 tion seems to be not very effective for a high deposition rate as
 268 Ti and Al targets were sputtered from opposite directions.
 269 Most of the previous literature indicates the use of four or
 270 six target machines.

271 Table 3 shows the chemical composition of the as-
 272 deposited coatings obtained through bulk EDX analysis.
 273 For pure targets (samples S7, S8 and S9), $\left(\frac{Al}{Ti+Al}\right) \times 100$
 274 ratio seems to be slightly more than 55, indicating this to be

275 an Al-rich coating. This may be attributed to the higher target
 276 current density used for aluminium (4 A as opposed to 3 A for
 277 Ti targets). Oliveira et al. [20] reported the $\left(\frac{Al}{Ti+Al}\right) \times 100$ ratio
 278 to be 34.5 % for an aluminium target current of 1.75 A against
 279 a total operating current of 10.5 A, and an increase in the
 280 aluminium target current led to an increase in this ratio. While
 281 using alloyed targets, the same ratio was found to be around
 282 36 in the present work, which almost indicates a transfer of the
 283 alloying percentage of the target to the coating despite reactive
 284 sputtering.

285 Table 4 summarizes the important coating characteristics.
 286 For a 9-h-long coating cycle, around 2 μm coating could be
 287 obtained from pure targets, providing a deposition rate of
 288 only 3.7 nm/min, whereas a coating thickness in excess of
 289 12 μm could be obtained using alloyed targets. Thus, the
 290 deposition rate is around 22 nm/min when alloyed targets
 291 are used. Astrand et al. [21] reported a similar deposition
 292 rate (23 nm/min) for TiAlN coating using four pure targets
 293 in a pulsed DC CFUBMS system.

294 The composite Vicker’s micro-hardness for TiAlN coat-
 295 ing has been measured to be just better than 21 GPa for pure
 296 targets. The literature indicates similar composite micro-
 297 hardness to be as much as 30–40 GPa. For example, Oli-
 298 veira et al. [22] reported a depth-sensing indentation hard-
 299 ness of 36 GPa for TiAlN film at a measurement load of
 300 only 20 mN. Mushil and Hruby [9] similarly obtained a
 301 micro-hardness of better than 40 GPa with a indentation
 302 load of 15 mN. A nano-hardness of around 31 GPa was
 303 reported separately by Shum et al. [23] and Zywitzki et al.
 304 [24]. This may be attributed to a significant substrate effect
 305 as 1 N load was used for indentation in the present investi-
 306 gation. Any reduction in load led to a very small indenta-
 307 tion, which prompted the choice of 1 N as the indentation
 308 load. The use of alloyed target provided composite micro-
 309 hardness values of around 21 GPa (S10) and 34 GPa (S11).



Q6 Fig. 2 Surface morphology and fractograph of coatings—S8, S10 and S11

t3.1 **Table 3** Chemical composition of the as-deposited TiAlN coatings

t3.2

t3.3

Sample no.	Atomic percentage of elements				$\left(\frac{Al}{Ti+Al}\right)$
	Ti	Al	N	Fe	
t3.4 S7	22.08	28.50	48.63	0.79	56.35
t3.5 S8	22.14	29.02	48.2	0.63	56.72
t3.6 S9	21.39	27.92	50.12	0.57	56.62
t3.7 S10	36.59	23.08	40.33	0.0	36.68
t3.8 S11	38.57	20.93	40.50	0.0	35.18

This clearly indicates the beneficial effect of a higher deposition frequency on the hardness of the coating as the same was 300 kHz for S11 compared to 200 kHz for S10. As the coatings are rather thick for samples S10 and S11, these two hardness values can be viewed as the coating hardness as the effect of the substrate is expected to be not very significant.

A hard wear-resistant coating also needs to have sufficient adhesion with the substrate for any useful application as a cutting tool. The effect of the type of target on the adhesion of the coating could not be captured in the present study, but a minimum critical load of around 51 N and a

310
311Q8
312
313
314
315
316
317
318
319
320

Table 4 Coating properties of the as-deposited TiAlN coatings

Sample no.	Mechanical properties of coating			
	Coating thickness (μm)	Composite micro-hardness (GPa)	Critical load (N)	Wear coefficient (×10 ⁻¹⁵ m ³ /Nm)
S7	2.18±0.01	22.54±4.19	60±15	5.63±0.97
S8	1.87±0.23	22.11±4.88	77.5±12.5	8.69±1.19
S9	2.06±0.06	21.69±5.39	70±15	9.52±1.19
S10	10.1±0.25	21.71±2.8	51.1±7	26.1±6.4
S11	12.5±5.00	34.7±6.29	86±4	27.2±6.4

maximum critical load of around 86 N were obtained for the whole experimental domain, as detailed in Table 4. TiN coatings deposited using a similar route provided lower critical load [19], whereas TiN–MoS_x coating yielded critical load in the range of 50–60 N [25]. Shum et al. [23] also reported around 70 N critical load for TiAlN coatings deposited using pure targets in a four-target machine.

The tribological performance of the coating has been accessed by the wear coefficient. The wear coefficient has been determined as the ratio of the total volume of the wear track to the product of normal load and sliding distance. A lower wear coefficient indicates better wear resistance of the coating in a ball-on-disc configuration. This configuration primarily simulates adhesion-diffusive wear. However, the ball-on-disc test may also lead to a scenario of three-body abrasion if the hard coating fragments during the test; a similar situation has been reported by Grzesik et al. [26]. TiN coatings provide wear coefficients as low as 6 × 10⁻¹⁵–10 × 10⁻¹⁵ m³/Nm. For the TiN–MoS_x composite coating, the same could be as low as 0.5 × 10⁻¹⁵ m³/Nm [25]. Similarly, wear coefficients of around 10 × 10⁻¹⁵ m³/Nm [27] or even in the range of 20 × 10⁻¹⁵–80 × 10⁻¹⁵ m³/Nm [28] have been reported for TiAlN coatings. In the present study, the coatings obtained from pure targets provided wear resistance in the range of 5.6–9.5 × 10⁻¹⁵ m³/Nm, which is better than the reported values. Though the coatings obtained using alloyed targets provided better coating thickness, higher composite micro-hardness and higher critical load (for sample S11), such coatings yielded poor wear resistance, as has been noted in Table 4. Such a high value of wear coefficient (26 × 10⁻¹⁵ m³/Nm) could be attributed to the possible removal of overgrowths, as seen in Fig. 2, during the ball-on-disc test.

Machining performance can be evaluated by assessing different machinability criteria, namely, cutting forces, cutting temperature, product quality, tool wear, etc. Tool wear and tool life are the most important machinability criteria having direct industrial relevance. In the present work, the machining performance of the coated inserts has been primarily evaluated using the tool wear criterion. Dry turning has been performed as dry machining is gradually becoming

more industrially relevant [29]. Figure 3 shows the growth of average flank wear against machining time whilst dry turning SAE 1020 steel bar of 160-mm diameter at a cutting speed of 250 m/min, feed of 0.2 mm/rev and a depth of cut of 2 mm. Though the break-in wear performance of all the inserts looks very similar, the beneficial effect of using alloyed targets becomes very evident after around 100 s of machining. The average flank wear as well as the rate of growth of flank wear for samples S10 and S11 (obtained using alloyed target) are significantly better than the coated tools obtained using pure targets. The literature suggests that a high coating thickness may not be suitable for machining as the coating may spall due to lack of toughness. Posti and Nieminen [30] noted that the tool life increased in turning up to a maximum coating thickness of 6 μm, and the same increase was noted with coating thickness around 2–3 μm in the case of interrupted cutting. A similar effect of coating thickness has been reported by Tuffy et al. [31] for TiN deposited using CFUBMS. Thus, one may infer that alloyed targets have provided thicker coatings and that the thickness of the coating has played a significant beneficial role in

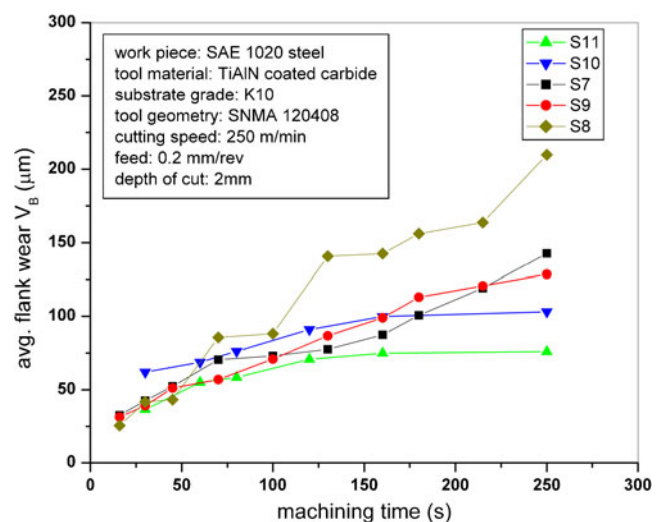
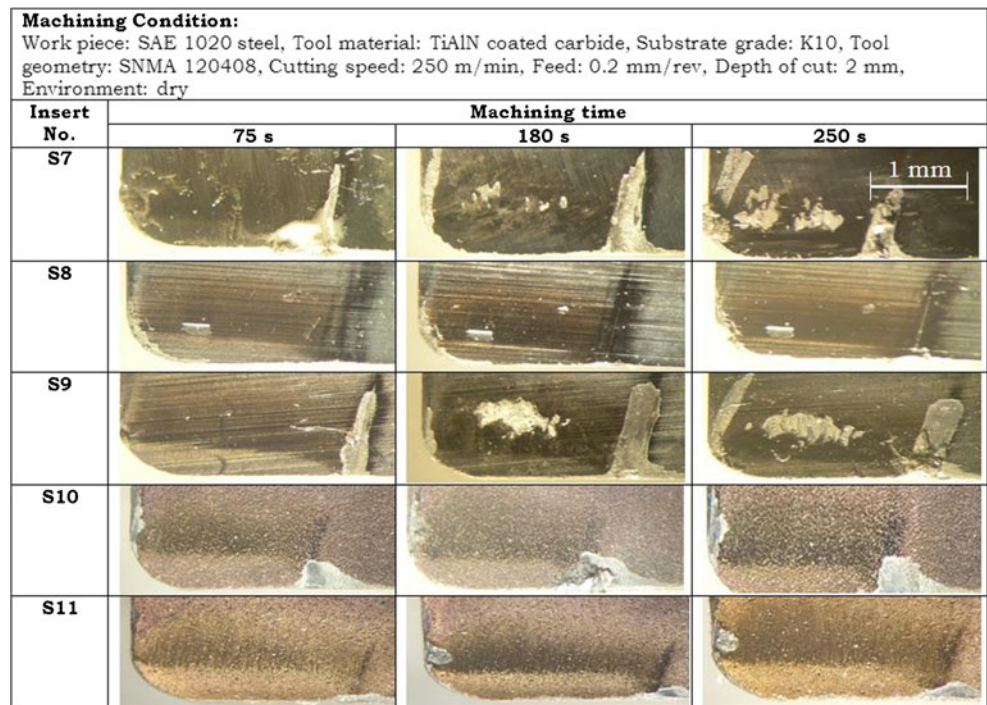


Fig. 3 Growth of average flank wear against machining time whilst dry turning of SAE 1020 steel at a cutting speed of 250 m/min, feed of 0.2 mm/rev and a depth of cut of 2 mm

Fig. 4 Nature and extent of crater wear of different inserts after dry turning of SAE 1020 steel at a cutting speed of 250 m/min, feed of 0.2 mm/rev and a depth of cut of 2 mm



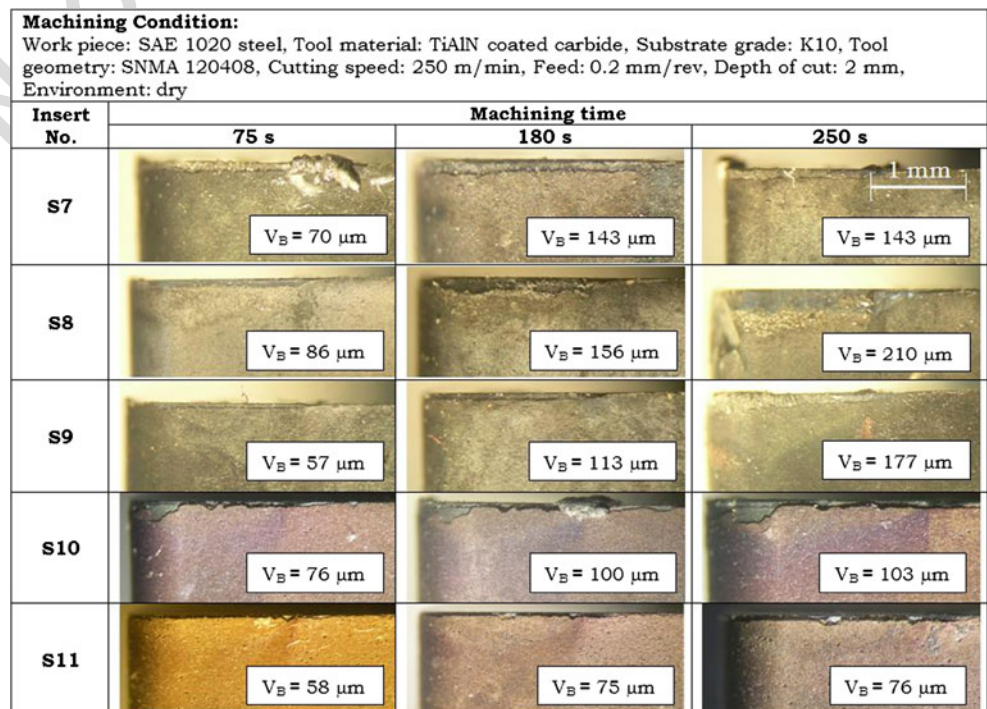
383 improving wear resistance of the coated tool during the dry
 384 turning despite opposing views expressed in the literature.
 385 Interestingly, the performance of sample S11 is even better
 386 than sample S10. This may be attributed to the benefit of a
 387 higher target frequency on the coating characteristics, as
 388 documented by Kelly and Arnell [32] and Bhaduri et al.
 389 [19]. In the present study also, sample S11 provided higher
 390 composite micro-hardness and critical load as compared to

sample S10, which may have as well contributed to its better
 machining performance.

The nature and the extent of crater wear and flank wear
 on different inserts after dry turning of SAE 1020 steel have
 been revealed in Figs. 4 and 5, respectively. It may be
 emphasized that the photomicrographs have been taken after
 cleaning the inserts in acidic solution. Inserts coated using
 pure targets (S7, S8 and S9) started developing main

391
 392
 393
 394
 395
 396
 397
 398

Fig. 5 Nature and extent of flank wear of different inserts after dry turning of SAE 1020 steel at a cutting speed of 250 m/min, feed of 0.2 mm/rev and a depth of cut of 2 mm



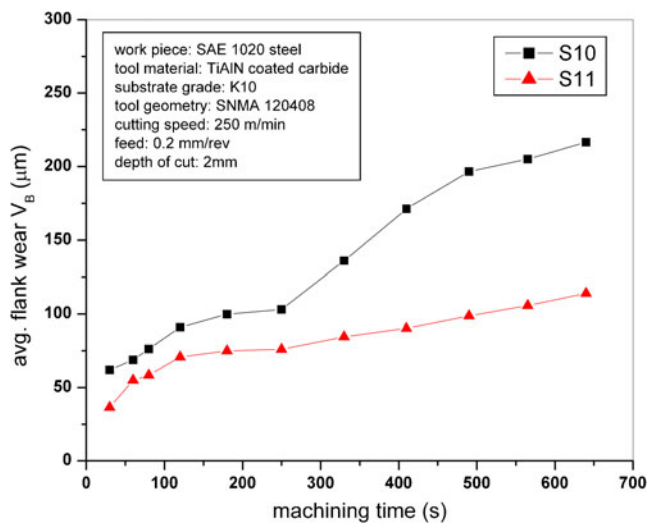


Fig. 6 Growth of average flank wear of inserts S10 and S11 against the machining time whilst dry turning of SAE 1020 steel at a cutting speed of 250 m/min, feed of 0.2 mm/rev and a depth of cut of 2 mm

399 grooving wear on the rake surface within 75 s of machining.
 400 For all the above three inserts, partial removal of coating
 401 from the crater surface also started appearing within 180 s.
 402 There has also been the appearance of auxiliary grooving
 403 wear on the rake surface. Sample S10 (obtained from
 404 alloyed target at 200-kHz target frequency) did show
 405 removal of the coating at the location of the grooving
 406 wear after 75 s of machining, but its extent has been
 407 significantly less compared to inserts S7, S8 and S9.
 408 S11 (obtained from alloyed target at 300-kHz target fre-
 409 quency) clearly shows suppression of the development of
 410 primary grooving wear or removal of the coating even
 411 after machining for 250 s, exhibiting once again the
 412 benefit of a higher target frequency.

413 Figure 5 clearly reveals the tendency of material built-up
 414 on the cutting edge, particularly for S7 inserts, which could
 415 not be removed even by acid etching. Flank wear seems to
 416 be uniform, but in excess of 140 μm on inserts coated using
 417 pure targets. For example, S8 yielded an average flank wear

of 210 μm after 250 s of machining. Insert S10 (obtained 418
 from alloyed target at a 200-kHz target frequency), after 419
 250 s of machining, provided 103 μm of average flank wear, 420
 but the coating was removed toward the nose of the tool. It 421
 seems flank wear has developed more because of coating 422
 removal rather than abrasion, indicating poor adhesion be- 423
 tween the coating and the substrate. Furthermore, lack of 424
 coating toughness could also be the reason for such coating 425
 removal from the flank surface, as has been mentioned 426
 earlier by Posti and Nieminen [30] and Tuffy et al. [31]. 427
 S11, on the other hand, provided a flank wear of only 76 μm 428
 after 250 s of machining. 429

Superior machining performance of samples S10 and S11 430
 is clearly revealed in Figs. 3, 4 and 5 in dry turning. Thus, it 431
 was decided to continue dry turning of SAE 1020 steel with 432
 only these two inserts up to 640 s; the growth of average 433
 flank wear on S10 and S11 inserts has been shown in Fig. 6. 434
 The excellent machining performance of S11 is clearly 435
 visible in Fig. 6, when it provided average flank wear of 436
 only 114 μm after almost 11 min of machining. 437

No literature could be found to directly compare the present 438
 result. Jindal et al. [7] reported the comparative performance 439
 of different PVD-coated tools in the machining of SAE 1045 440
 steel, which is also a plain carbon steel but with a nominal 441
 carbon percentage of 0.45 %. They obtained tool life in excess 442
 of 1 h when the insert was coated with TiAlN coating using a 443
 magnetron sputtering process. It may be mentioned that they 444
 used the tool life criterion of 0.4 mm of average flank wear. 445
 The chosen cutting velocity was 305 m/min, which is 22% 446
 more than the present cutting velocity. But the feed and depth 447
 of cut were significantly less, by around 25 and 62 %, respec- 448
 tively. The material removal rate (MRR) was only 34 % of the 449
 MRR in the present study. Moreover, they employed a coolant 450
 during machining. Khrais and Lin [8] investigated the wear 451
 mechanism of commercial TiAlN PVD-coated inserts whilst 452
 dry machining AISI 4140 steel, which is a low-alloy steel 453
 having a carbon percentage of 0.4 % with nickel (0.1 %) and 454
 molybdenum (0.2 %) as alloying elements. Dry turning at a 455
 cutting velocity of 260 m/min yielded a tool life of around 456

Table 5 Comparative machining performance

Time	$V_{B_{max}}$ (mm)	Max. flank wear rate ($\times 10^{-6}$ mm/s)	MRR (mm^3/s)	MRR/wear rate ($\times 10^6$ mm^2)	Carbon equiv. CE	$MRR \times CE / \text{wear rate}$ ($\times 10^6$ mm^2)
Khrais and Lin: AISI 4140 steel as work material with feed of 0.14 mm/rev and depth of cut of 1 mm						
310 m/min	10 min	0.55	900	723.33	0.79	0.567
260 m/min	20 min	0.33	200	606.67	2.18	1.236
	25 min	0.61	400	606.67	1.48	0.839
210 m/min	10 min	0.09	100	490	3.15	1.786
	20 min	0.11	92.6	490	5.29	2.999
SAE 1020 steel as work material with cutting velocity of 250 m/min, feed of 0.2 mm/rev and depth of cut of 2 mm						
S11 250 m/min	10 min, 40 s	0.203	0.0003	1,666.67	5.26	0.332
						1.746

Fig. 7 Nature and extent of crater and flank wear of different inserts after 120 s of dry turning of SAE 1070 steel at a cutting speed of 160 m/min, feed of 0.2 mm/rev and a depth of cut of 2 mm

Machining Condition:	Insert No.	Rake Face	Flank Face
		Work piece: SAE 1070 steel Tool material: TiAlN coated carbide Substrate grade: K10 Tool geometry: SNMA 120408 Cutting speed: 160 m/min Feed: 0.2 mm/rev Depth of cut: 2 mm Environment: dry Cutting time: 120 s	S7
	S9		 V _B = 449 μm
	S10		 V _B = 77 μm
	S11		 V _B = 76 μm

457 22 min for a tool life criterion of 0.6 mm of maximum flank
458 wear. They employed a depth of cut of 1 mm (50 % less than
459 the present depth of cut) and a feed of 0.14 mm/rev (30 % less
460 than the present feed).

461 To enable a more meaningful comparison between the
462 cutting performances of the present coated inserts with the
463 same from the literature, the following strategy has been
464 adopted. In grinding, resistance to wheel wear is evaluated
465 using a grinding ratio, which is the ratio of the material
466 removal rate to the wear rate [33]. Similarly, Table 5
467 presents the ratio of the material removal rate to the rate of
468 growth of maximum flank wear. For benchmarking, data
469 from Khrais and Lin [8] have been used as they have also
470 undertaken dry turning. The said ratio has been varied
471 between 0.79 and 5.29×10^6 mm² for different cutting ve-
472 locities at different stages of machining, as has been

473 extracted from the work of Khrais and Lin [8]. The same 473
474 ratio is as much as 5.26×10^6 mm² for the present TiAlN- 474
475 coated insert (S11). This indicates competitive performance 475
476 of the presently developed inserts with respect to the 476
477 machining performance available in the literature. 477

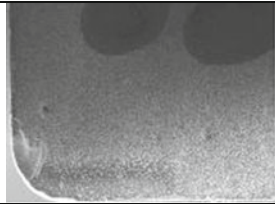
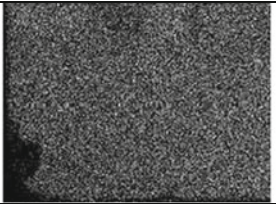
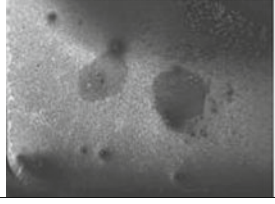
478 However, one may argue that two work materials are 478
479 different. Carbon equivalent has been used for a long time 479
480 in area welding to judge the hardenability and hardness of 480
481 weldment of plain and low-carbon steels. This approach 481
482 allows a comparison of the results even if the steels are of 482
483 different chemical compositions [34]. The concept of carbon 483
484 equivalent has also been used in machining by Capello [35]. 484
485 A higher carbon equivalent would indicate the availability 485
486 of more carbide-forming elements and more tool wear 486
487 during machining. Thus, the above proposed ratio of the 487
488 material removal rate to the rate of growth of maximum 488

Fig. 8 Nature and extent of crater and flank wear of S10 and S11 after 200 s of dry turning of SAE 1070 steel at a cutting speed of 160 m/min, feed of 0.2 mm/rev and a depth of cut of 2 mm

Insert No.	Coated surface	Machining Condition:		
		Work piece: SAE 1070 steel, Tool material: TiAlN coated carbide, Substrate grade: K10, Tool geometry: SNMA 120408, Cutting speed: 160 m/min, Feed: 0.2 mm/rev, Depth of cut: 2 mm, Environment: dry		
		Machining Time		
		45 s	120 s	200 s
S10	Rake			
	Flank	 V _B = 57 μm	 V _B = 77 μm	 V _B = 155 μm
S11	Rake			
	Flank	 V _B = 52 μm	 V _B = 76 μm	 V _B = 98 μm

Q14

Fig. 9 Elemental area mapping on inserts S10 and S11 after 120 s of dry turning of SAE 1070 steel at a cutting speed of 160 m/min, feed of 0.2 mm/rev and a depth of cut of 2 mm

Insert No.	Overview	Ti	Al
S10			
S11			

489 flank wear is re-modified by multiplying the same by the
 490 carbon equivalent. This proposes taking care of the dif-
 491 ference in the chemical compositions in the work mater-
 492 ial. Table 5 indicates the modified ratio which varied
 493 between 0.448 and 2.999×10^6 mm² for the work un-
 494 dertaken by Khrais and Lin [8]. The same ratio has been
 495 found to be 1.746×10^6 mm² in the present case. Thus,
 496 one may infer that the present cutting tools coated using
 497 alloyed targets (particularly sample S11) are very similar
 498 in performance to commercially coated inserts despite
 499 being deposited in a dual-cathode system.

500 In the present work, dry turning of SAE 1070 steel was
 501 also conducted at a cutting velocity of 160 m/min with a
 502 feed and depth of cut of 0.2 mm/rev and 2 mm, respectively.
 503 Figure 7 shows the nature and extent of flank and crater
 504 wear on selected inserts after 120 s of machining. Overall,
 505 inserts coated using alloyed targets are far superior in ma-
 506 chining performance. S11 once again establishes its better
 507 performance compared to the other inserts. This is also
 508 clearly visible in Fig. 8 when machining was continued until
 509 200 s. Figure 9 shows the elemental area mapping on S10
 510 and S11 inserts after 120 s of machining. It is evident that
 511 the coating has not been removed from the rake surface of
 512 S11 and has only been partially damaged on the rake surface
 513 of S10.

514 **4 Conclusion**

515 TiAlN coating could be successfully deposited on uncoated
 516 carbide inserts using both pure and alloyed targets via dual-
 517 cathode, pulsed DC reactive unbalanced sputtering route.
 518 Pure targets provided coating thickness in the range of
 519 2 μm, whereas coating thickness in excess of 12 μm could
 520 be obtained from alloyed targets.

521 The scratch test provided critical load in the range of 50–
 522 90 N, though the effect of the type of target was not evident.
 523 Wear coefficients as obtained by the ball-on-disc tribological

test is acceptably low in the range of $5-9 \times 10^{-15}$ m³/Nm for
 coatings from pure targets. Coatings deposited from alloyed
 targets yielded poor wear coefficients in the ball-on-disc tri-
 biological test.

SAE 1020 steel bar could be efficiently dry turned at
 250 m/min for more than 4 min with all the inserts. How-
 ever, the average flank wear on the coated inserts obtained
 from alloyed targets was substantially less than that on
 inserts coated using pure targets. When machining was
 continued until almost 11 min, one of the inserts only
 underwent an average flank wear of around 115 μm. Such
 machining performance is comparable to previously
 reported ones despite being deposited using dual-cathode
 deposition systems, unlike four- or six-cathode systems.

Even dry turning of SAE 1070 high-carbon steel at
 160 m/min did not yield more than 100 μm of average flank
 wear on the same insert coated using alloyed targets for a
 machining time of more than 3 min.

Acknowledgment The authors gratefully acknowledge the funding
 support received from the Department of Science and Technology,
 Government of India, under FIST programme (sanction no. SR/FST/
 ET-II-003/2000 dated 20.5.2002).

References

- Munz WD (1986) Titanium aluminium nitride films: a new alter-
 native to TiN coatings. *J Vac Sci Technol, A* 4:2717
- Lee KH, Park CH, Yoon YS, Lee JJ (2001) Structure and proper-
 ties of Ti Cr N coatings produced by the ion-plating method. *Thin
 Solid Films* 385:167–173
- Santana AE, Karimi A, Derflinger VH, Schutze A (2004) Thermal
 treatment effects on microstructure and mechanical properties of
 TiAlN thin films. *Tribol Let* 17(4):689–696
- McIntyre D, Greene JE, Hakansson G, Sundgren JE, Munz WD
 (1990) Oxidation of metastable single phase polycrystalline Ti_{0.5}
 Al_{0.5} N films: kinetics and mechanisms. *J Appl Phys* 67(3):1542–
 1553
- Hsieh JH, Liang C, Yu CH, Wu W (1998) Deposition and charac-
 terization of TiAlN and multi-layered TiN/TiAlN coatings using

563 unbalanced magnetron sputtering. *Surf Coat Technol* 108–
 564 109:132–137

565 6. Kelly PJ, Abu-Zeid OA, Arnell RD, Tomg J (1996) The deposition
 566 of aluminium oxide coatings by reactive unbalanced magnetron
 567 sputtering. *Surf Coat Technol* 86–87:28–32

568 7. Jindal PC, Santhanam AT, Schleinkofer U, Shuster AF (1999)
 569 Performance of PVD TiN, TiCN, and TiAlN coated cemented
 570 carbide tools in turning. *Int J Refract Met Hard Mater* 17:163–170

571 8. Khrais SK, Lin YJ (2007) Wear mechanisms and tool performance
 572 of TiAlN PVD coated inserts during machining of AISI 4140 steel.
 573 *Wear* 262:64–69

574 9. Musil J, Hruby H (2000) Superhard nanocomposite $Ti_{1-x}Al_xN$
 575 films prepared by magnetron sputtering. *Thin Solid Films*
 576 365:104–109

577 10. Zhou T, Nie P, Cai X, Chu PK (2009) Influence of N_2 partial
 578 pressure on mechanical properties of (Ti, Al)N films deposited by
 579 reactive magnetron sputtering. *Vacuum* 83:1057–1059

580 11. He Y, Apachitei I, Zhou J, Walstock T, Duszczuk J (2006) Effect of
 581 prior plasma nitriding applied to a hot-work tool steel on the
 582 scratch-resistant properties of PACVD TiBN and TiCN coatings.
 583 *Surf Coat Technol* 201:2534–2539

584 12. Chattopadhyay AK, Chattopadhyay AB (1984) Wear character-
 585 istics of ceramic cutting tools in machining steel. *Wear* 93:347–359

586 13. Chattopadhyay AK, Chattopadhyay AB (1982) Wear and perfor-
 587 mance of coated carbide and ceramic tool. *Wear* 80:239–258

588 14. Venkatesh VC, Ye CT, Quinto DT, Hoy DEP (1991) Performance
 589 studies of uncoated, CVD-coated and PVD-coated carbides in
 590 turning and milling. *CIRP Ann Manuf Technol* 40(1):545–550

591 15. Gekonde HO, Subramanian SV (2002) Tribology of tool–chip inter-
 592 face and tool wear mechanisms. *Surf Coat Technol* 149:151–160

593 16. Konyashin IY (1995) PVD/CVD technology for coating cemented
 594 carbides. *Surf Coat Technol* 71:277–283

595 17. Alberdi A, Margin M, Diaz B, Sanchez O, Escobar Galindo R
 596 (2007) Wear resistance of titanium–aluminium–chromium–nitride
 597 nanocomposite thin films. *Vacuum* 81:1453–1456

Q15 598 18. Veldhuis SC, Dosbaeva GK, Elfizy A, Fox-Rabinovich GS, Wagg
 599 T (2010) Investigations of white layer formation during machining
 600 of powder metallurgical Ni-based ME 16 superalloy. *J Mater Eng*
 601 *Perform* 19(7):1031–1036

602 19. Bhaduri D, Ghosh A, Gangopadhyay S, Paul S (2010) Effect of
 603 target frequency, bias voltage and bias frequency on microstructure
 604 and mechanical properties of pulsed DC CFUBM sputtered TiN
 605 coating. *Surf Coat Technol* 204:3684–3697

606 20. Oliveira JC, Manaia A, Cavaleiro A (2008) Hard amorphous Ti–Al–
 607 N coatings deposited by sputtering. *Thin Solid Films* 516:5032–5038

608 21. Astrand M, Selinder TI, Sjostrand ME (2005) Deposition of $Ti_{1-x}Al_xN$
 609 using bipolar pulsed dual magnetron sputtering. *Surf Coat*
 610 *Technol* 200:625–629

611 22. Oliveira JC, Manaia A, Dias JP, Cavaleiro A, Teer D, Taylor S
 612 (2006) The structure and hardness of magnetron sputtered Ti–Al–
 613 N thin films with low N contents (<42%). *Surf Coat Technol*
 614 200:6583–6587

615 23. Shum PW, Li KY, Zhou ZF, Shen YG (2004) Structural and
 616 mechanical properties of titanium–aluminium–nitride films depos-
 617 ited by reactive closed-field unbalanced magnetron sputtering.
 618 *Surf Coat Technol* 185:245–253

619 24. Zywitzki O, Klostermann H, Fietzke F, Modes T (2006) Structure
 620 of superhard nanocrystalline (Ti, Al)N layers deposited by reactive
 621 pulsed magnetron sputtering. *Surf Coat Technol* 200:6522–6526

622 25. Gangopadhyay S, Acharya R, Chattopadhyay AK, Paul S (2009)
 623 Composition and structure–property relationship of low friction,
 624 wear resistant TiN– MoS_x composite coating deposited by pulsed
 625 closed-field unbalanced magnetron sputtering. *Surf Coat Technol*
 626 203:1565–1572

627 26. Grzesik W, Zalisz Z, Krol S, Nieslony P (2006) Investigation on
 628 friction and wear mechanisms of the PVD–TiAlN coated carbide in
 629 dry sliding against steel and cast iron. *Wear* 261:1191–1200

630 27. Mo JL, Zhu MH, Lei B, Leng YX, Huang N (2007) Comparison of
 631 tribological behaviours of AlCrN and TiAlN coatings—deposited
 632 by physical vapour deposition. *Wear* 263:1423–1429

633 28. Li X, Li C, Zhang Y, Tang H, Li G, Mo C (2010) Tribological
 634 properties of the Ti–Al–N thin films with different components
 635 fabricated by double-targeted co-sputtering. *Appl Surf Sci*
 636 256:4272–4279

637 29. Klocke F, Eisenblatter G (1997) Dry cutting. *CIRP Ann Manuf*
 638 *Technol* 46(2):519–526

639 30. Posti E, Nieminen I (1989) Influence of coating thickness on the life
 640 of TiN-coated high speed steel cutting tools. *Wear* 129:273–283

641 31. Tuffy K, Byrne G, Dowling D (2004) Determination of the opti-
 642 mum TiN coating thickness on WC inserts for machining carbon
 643 steel. *J Mater Process Technol* 155–156:1861–1866

644 32. Kelly PJ, Arnell RD (2000) Magnetron sputtering: a review of
 645 recent developments and applications. *Vacuum* 56:159–172

646 33. Malkin S (1989) Grinding technology—theory and applications of
 647 machining with abrasives. Society of Manufacturing Engineers,
 648 Michigan

649 34. Lancaster JF (1999) Metallurgy of welding. Abington Publishing,
 650 Cambridge

651 35. Capello E (2006) Residual stresses in turning: part II. Influence of
 652 the machined material. *J Mater Process Technol* 172:319–326

AUTHOR QUERIES

AUTHOR PLEASE ANSWER ALL QUERIES.

- Q1. Please check captured corresponding author if appropriate.
- Q2. Occurrences of “dc” were changed to “DC”. Please check.
- Q3. Please check value here if appropriately presented.
- Q4. Please check presentation of this entry if appropriate.
- Q5. Please check changes made to this sentence.
- Q6. Figures 2,4,5 & 8 contains small and blurry text. Please provide better quality of image, otherwise, please advise if okay to proceed as is.
- Q7. Please check change made here.
- Q8. Please check whether this sentence is appropriately presented.
- Q9. “tool life increased in turning upto a maximum coating thickness of 6 m and the same was around 2–3 m in case of interrupted cutting” was changed to “tool life increased in turning up to a maximum coating thickness of 6 μm , and the same increase was noted with coating thickness around 2–3 μm in the case of interrupted cutting”. Please check.
- Q10. Please check changes made to this sentence.
- Q11. Please check merging made here if appropriate.
- Q12. Please check changes made here.
- Q13. Please check change in sentence presentation made here.
- Q14. Figure 9 has discrepancy between pdf and tiff file, we proceed using pdf file since it has vector objects/text.
- Q15. Ref. 18 was not cited anywhere in the text. Please provide a citation. Alternatively, delete the item from the list.